

The measurement of R at CLEO

J. Libby^a (on behalf of the CLEO collaboration)

^aUniversity of Oxford, Denys Wilkinson Building, Keble Road, Oxford, OX1 3RH, United Kingdom

Measurements of the total cross section of $e^+e^- \rightarrow$ hadrons are presented in two different ranges of centre-of-mass energy. The measurements are made using the CLEO III and CLEO-c detectors at the Cornell Electron Storage Ring. The absolute cross sections and the values of R , the ratio of hadronic to muon pair production cross sections, are determined at seven centre-of-mass energies between 6.964 and 10.538 GeV. The total cross sections and values of R are also determined at thirteen centre-of-mass energies between 3.97 and 4.26 GeV; in addition, the inclusive and exclusive cross sections for D^+ , D^0 and D_s^+ production are presented. Furthermore, for the lower centre-of-mass energy range, exclusive cross-sections are presented for final states consisting of two charm mesons: $D\bar{D}$, $D^*\bar{D}$, $D\bar{D}^*$, $D^*\bar{D}^*$, $D_s^+D_s^-$, $D_s^{*+}D_s^-$, $D_s^+D_s^{*-}$, $D\bar{D}^*\pi$ and $D^*\bar{D}^*\pi$.

1. Introduction

The determination of R , the ratio of the radiation-corrected hadronic cross section to the calculated lowest-order cross section for muon pair production is presented in two ranges of centre-of-mass energy, \sqrt{s} . The motivation for these studies is different in the two \sqrt{s} ranges.

The measurements of R at seven values of \sqrt{s} between 6.964 and 10.538 GeV test the asymptotic freedom of the QCD coupling α_s in the range of \sqrt{s} where u , d , s and c , quarks are produced. The values of α_s are extracted by comparing the measurements of R to a perturbative QCD calculation at the four-loop level [1].

Measurements of R in the region just above the $c\bar{c}$ threshold ($\sqrt{s} = 3.970$ to 4.260 GeV) exhibit a rich structure (for example see Ref. [2]); this reflects the production of $c\bar{c}$ resonances. Interesting features include an enhancement at $D^*\bar{D}^*$ threshold ($\sqrt{s} = 4.02$ GeV) and a broad plateau beginning at the $D_s^{*+}D_s^-$ threshold ($\sqrt{s} = 4.08$ GeV). There is considerable theoretical interest in the composition of these enhancements [3]. However, there is limited experimental information available which motivates the exclusive cross sections presented in this paper. The following final states are considered: $D\bar{D}$, $D^*\bar{D}$, $D\bar{D}^*$, $D^*\bar{D}^*$, $D_s^+D_s^-$, $D_s^{*+}D_s^-$ and $D_s^+D_s^{*-}$, $D\bar{D}^*\pi$ and $D^*\bar{D}^*\pi$. The total cross sections and values of R are also de-

termined at the thirteen points studies.

The results given in this paper are presented in greater detail elsewhere [4,5].

2. CLEO III and CLEO-c

All measurements presented are made with data collected at the Cornell Electron Storage Ring (CESR). The CLEO III detector [6] is used to study the data with $\sqrt{s} = 6.964 - 10.538$ GeV. The CLEO-c detector [7] is used to study the data around $c\bar{c}$ threshold. The principal differences between the CLEO III and CLEO-c detectors are the reduction in solenoid field from 1.5 to 1.0 T and the replacement of CLEO III's four-layer silicon-strip detector by a six-layer all-stereo inner drift chamber. These modifications improve the reconstruction of low momentum charged particles.

3. Measurements of R at $\sqrt{s} = 6.964 - 10.538$ GeV

The values of \sqrt{s} and integrated luminosities, $\int \mathcal{L} dt$, for each data point are given in Table 1. Hadronic events are selected from these data by placing criteria on individual tracks and showers, as well as the whole event.

Tracks used in the analysis are required to be of good quality, originate from close to the interaction point and have a momentum between 1

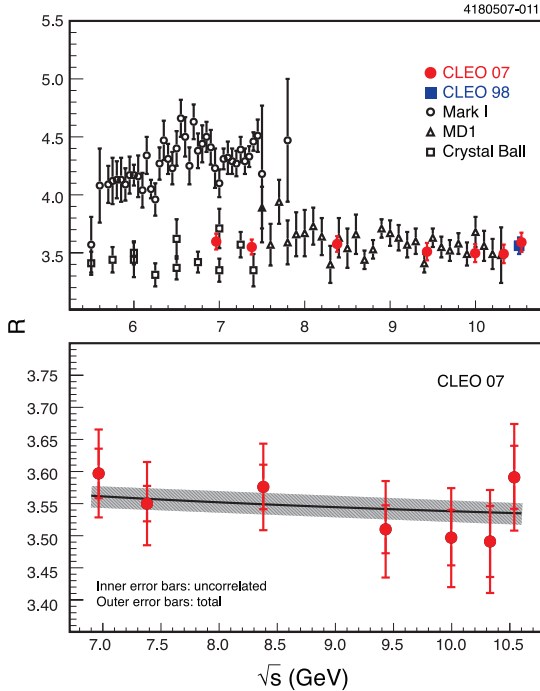


Figure 1. The upper figure compares the measurements of R presented in this paper with previous measurements. The lower plot compares the results with predicted values of R ; the width of band is given by the uncorrelated uncertainties on Λ .

and 150% of the beam momentum. Showers must have at least 1% of the beam momentum and not be associated with a track.

Several event variables are used to discriminate against background. The average point of origin of all tracks along the beam direction is used to reject beam-gas, beam-wall and cosmic ray events. The total visible energy normalised to twice the beam energy and the missing momentum in the beam direction normalised to the visible energy are used to remove two-photon and beam-gas events. Each event must contain at least four charged tracks and pass an event shape criteria to reject $e^+e^- \rightarrow l^+l^-$ ($l = e, \mu$ or τ) events. The ratio of total calorimeter energy associated to tracks and isolated showers normalised to twice the beam energy is used to reject Bhabha and tau-pair events. Initial state radiation events

Table 1

The centre-of-mass energy, luminosity and the value of R for the seven measurement points with $\sqrt{s} = 6.964 - 10.538$ GeV. The combined statistical and systematic uncertainty is given on the luminosity. The first, second and third uncertainties on R are the statistical, common systematic and uncorrelated systematic, respectively.

\sqrt{s} (GeV)	$\int \mathcal{L} dt$ (pb $^{-1}$)	R
10.538	904.50 ± 9.00	$3.591 \pm 0.003 \pm 0.067 \pm 0.049$
10.330	149.80 ± 1.60	$3.491 \pm 0.006 \pm 0.058 \pm 0.055$
9.996	432.60 ± 4.80	$3.497 \pm 0.004 \pm 0.064 \pm 0.043$
9.432	183.00 ± 2.00	$3.510 \pm 0.005 \pm 0.066 \pm 0.037$
8.380	6.78 ± 0.06	$3.576 \pm 0.024 \pm 0.058 \pm 0.025$
7.380	8.48 ± 0.07	$3.550 \pm 0.019 \pm 0.058 \pm 0.020$
6.964	2.52 ± 0.02	$3.597 \pm 0.033 \pm 0.057 \pm 0.020$

are removed by a criterion on the ratio of the maximum isolated shower energy normalised to the beam energy.

The efficiency of the selection increases from 82.1% at $\sqrt{s} = 6.964$ GeV to 87.4% at $\sqrt{s} = 10.538$. The dominant background remaining after the event selection is from $e^+e^- \rightarrow \tau^+\tau^-$ events, which is estimated from simulation. Other remaining backgrounds are estimated to give contributions smaller than the systematic uncertainty assigned to the event selection.

Radiative corrections must be applied to the measured total hadronic cross section to determine R . Corrections are applied for soft photon radiation and vacuum polarisation. In addition, corrections are applied for hard initial state radiation to the continuum and lower mass $q\bar{q}$ resonances. Furthermore, at three energy points, a correction is applied for the interference between a nearby Υ resonance and the continuum.

Several sources of significant systematic uncertainty are considered: luminosity, radiative corrections, multiplicity corrections and event selection criteria. The relative uncertainty on the luminosity is between 0.9% and 1.1% depending on \sqrt{s} . The uncertainty from the radiative corrections is dominated by those for the hadronic vacuum polarisation, which has an uncertainty of 1.0%. Some disagreement is found comparing the charged track multiplicity distribution in

data and simulation. Therefore, the efficiency is determined as a function of multiplicity before applying to the data. This procedure is estimated to have an uncertainty between 0.4% and 1.4% depending on \sqrt{s} . The uncertainty related to other selection criteria is estimated to be between 1.0 and 1.4% depending on \sqrt{s} .

The measured values of R are given in Table 1 along with the associated uncertainties. The total relative systematic uncertainty at each point is between 1.7 and 2.3%. The measured values are compared to previous measurements [8] in the upper plot in Figure 1. The measurements are in agreement with the results from Crystal Ball, MD1 and CLEO; however, they do not agree with the MARK I results.

The value of α_s is determined at each point using a perturbative QCD calculation of R at the four-loop level [1]. (This calculation ignores the quark masses; a determination including quark mass effects is presented in Ref. [9].) The compatibility of these measurements with others of α_s is evaluated by exploiting the expected running of α_s [10], which depends on the QCD scale Λ . The measured values determine $\Lambda = 0.31^{+0.09+0.29}_{-0.08-0.21}$ GeV and $\alpha(M_Z^2) = 0.126 \pm 0.005^{+0.015}_{-0.011}$, where the first uncertainties are statistical and the second systematic. These results agree with the world averages [11]. The lower plot in Figure 1 compares the measured values of R to those predicted by the fitted value of Λ .

4. Studies of exclusive charm and total cross sections at $\sqrt{s} = 3.97 - 4.26$ GeV

Data collected at thirteen energy points between $\sqrt{s} = 3.97 - 4.26$ GeV are studied. Specific criteria are used to select D^+ , D^0 and D_s^+ candidates; these closely follow other CLEO-c analyses [12]. The final states with the largest signal-to-background ratio are considered for $D^+ \rightarrow K^- \pi^+ \pi^+$ and $D^0 \rightarrow K^- \pi^+$. Eight decay modes are reconstructed to select D_s^+ candidates: $\phi(K^+ K^-) \pi^+$, $K^{*0}(K^- \pi^+) K^+$, $\eta(\gamma\gamma) \pi^+$, $\eta(\gamma\gamma) \rho^+(\pi^+ \pi^0)$, $\eta'(\pi^+ \pi^- \eta(\gamma\gamma)) \pi^+$, $\eta'(\pi^+ \pi^- \eta(\gamma\gamma)) \rho^+(\pi^+ \pi^0)$, $\phi(K^+ K^-) \rho^+(\pi^+ \pi^0)$ and $K_S^0(\pi^+ \pi^-) K^+$. These modes correspond to 16% of the total D_s^+ decay width.

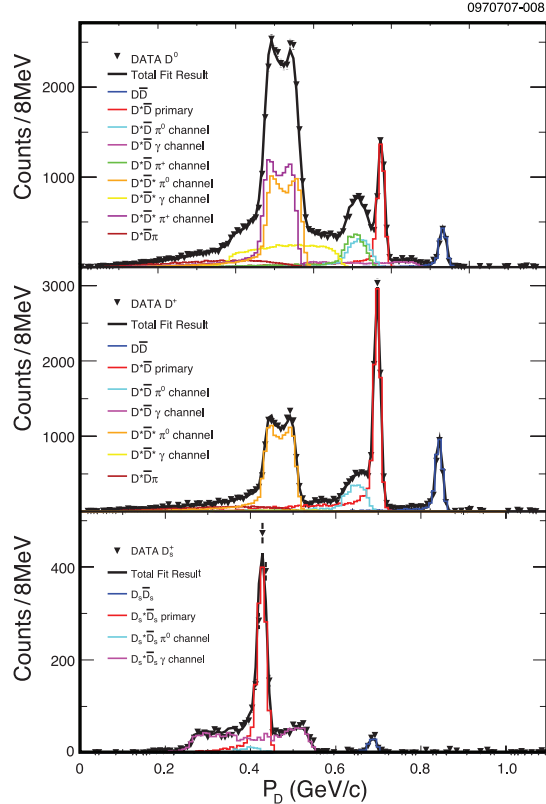


Figure 2. The sideband-subtracted momentum spectra for D^0 (upper), D^+ (middle) and D_s^+ (lower) for data collected at $\sqrt{s} = 4.17$ GeV. The fit results for the different production mechanisms are also shown.

Candidates are selected if their mass lies within ± 15 MeV of the nominal $D_{(s)}$ values. Background is subtracted using yields measured in $D_{(s)}$ mass sidebands extrapolated into the signal region. The momentum distribution of the $D_{(s)}$ candidates is then used to determine the production mechanism. The D^0 , D^+ and $D_s^+ \rightarrow \phi \pi^+$ momentum distribution at $\sqrt{s} = 4.17$ GeV is shown in Figure 2. The different peaks correspond to different production mechanisms. The shape of distributions for the individual processes are determined from simulation. The data are fit to the different components to determine the yields. For D^+ and D^0 production these are then corrected for efficiency, branching ratios and

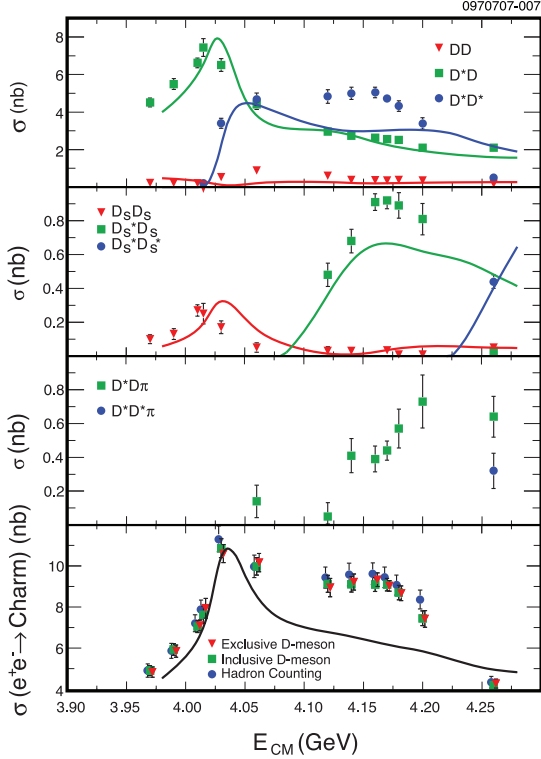


Figure 3. The production cross sections for $D^{(*)}\overline{D}^{(*)}$ (upper), $D_s^{(*)}\overline{D}_s^{(*)}$ (upper middle) and multi-body (lower middle) production. The lower plot shows the total charm cross section determined by the alternate methods described in the text. The two-body and total production cross sections are compared to a model [14].

luminosity to give the cross sections shown in the two upper plots in Figure 3. Two additional components describing multi-body production $D^*\overline{D}^{(*)}\pi$ are required to describe the low momentum distribution at $\sqrt{s} > 4.06$ GeV. This is the first observation of multi-body production in the charm threshold region.

Given the relative simplicity of the $D_s^{(*)+}D_s^{(*)-}$ production and the limited statistics an alternative technique is used to determine the cross sections. The separation of the different mechanisms in the beam-energy difference ($\Delta E = E_{D_s} - E_{beam}$) and the beam-constrained mass ($M_{bc} = \sqrt{E_{beam}^2 - |\mathbf{P}_{D_s}|^2}$) plane is used. The

background is subtracted using ΔE and M_{bc} sidebands. The resulting cross sections are shown in the upper middle plot in Figure 3.

The dominant sources of systematic uncertainty are the selection efficiency, yield determination and the normalisation. Details of the uncertainty on the selection efficiency can be found in Ref. [12]. The signal functions for the determination of D^0 and D^+ production mechanisms depend on the modelling of initial state radiation and the helicity amplitudes for D^*D^* ; variations of these models over a broad range of assumptions leads to the systematic uncertainty. Variations in the M_{bc} and ΔE selection criteria are used to estimate the uncertainty related to signal extraction in the D_s modes. The uncertainty on the normalisation arises from that on the measured luminosity and the branching fractions of the modes reconstructed [13]. The total systematic uncertainties are between 3.4% and 6.8% for two-body production mechanisms; the multi-body production mechanisms $D^*\overline{D}\pi$ and $D^*\overline{D}^*\pi$ have systematic uncertainties of 12% and 25% uncertainties, respectively.

The results are compared to an updated calculation of Eichten *et al.* [14]. There is reasonable qualitative agreement for most two-body production mechanisms apart from $D^*\overline{D}^*$ production in the \sqrt{s} range 4.05 to 4.20 GeV.

The results at 4.26 GeV have the potential to study the nature of the $Y(4260)$. Hybrid charmonium [15] and tetraquark [16] interpretations suggest enhancements of some production mechanisms; no significant enhancements are observed disfavouring these models.

The sum of the exclusive cross sections should equal the total charm cross section. This has been tested with measurements using two inclusive techniques. The sum of inclusive cross sections for single D^0 , D^+ and D_s production divided by two is found to be in agreement with the total exclusive cross sections. In addition, the total hadronic cross section is determined in a manner similar to that described in Section 3. The light-quark production cross section is subtracted using measurements below $c\bar{c}$ threshold extrapolated with $1/s$ dependence. The total charm cross section from this method is found to

be in agreement with the other two techniques. The cross sections determined by each method are compared to each other and a model in the lower plot of Figure 3.

The total hadronic cross section is radiatively corrected [17] to obtain the measurements of R , which is shown in Figure 4. These measurements are more precise and in good agreement with previous measurements [2,18].

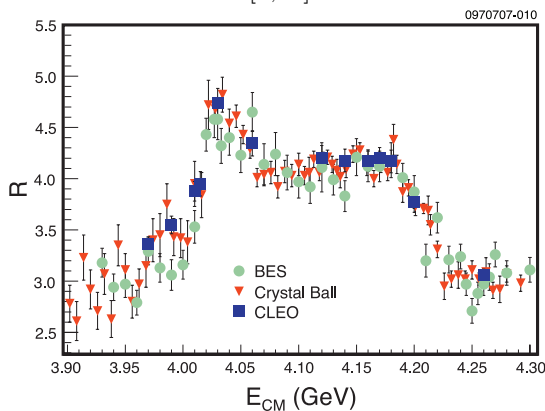


Figure 4. Measurements of R at thirteen points in the $c\bar{c}$ threshold region.

5. Conclusions

Seven measurements of R in the range $\sqrt{s} = 6.964 - 10.538$ GeV are used to determine a value of $\alpha_s(M_Z^2)$ in agreement with the world average. The exclusive and inclusive charm cross sections are measured at thirteen \sqrt{s} values near $c\bar{c}$ threshold. Multi-body production $D^* \overline{D^{(*)}} \pi$ is observed for the first time. All measurements of R are more precise and in agreement with earlier measurements.

REFERENCES

1. L. R. Surguladze and M. A. Samuel, Phys. Rev. Lett. **66**, 560 (1991); S. G. Gorishny, A. L. Kataev and S. A. Larin, Phys. Lett. B **259**, 144 (1991); M. Davier and A. Höcker, Phys. Lett. B **419**, 419 (1998).
2. J. Z. Bai *et al.*, Phys. Rev. Lett. **88**, 101802 (2002).
3. T. Barnes, J. Phys. Conf. Ser. **9**, 127 (2005); T. Barnes, arXiv:hep-ph/0406327; E. Eichten *et al.*, Phys. Rev. D **21**, 203 (1980); M. B. Voloshin, arXiv:hep-ph/0602233.
4. D. Besson *et al.*, Phys. Rev. D **76**, 072008 (2007).
5. D. Cronin-Hennessy *et al.*, arXiv:0801.3418 [hep-ex].
6. G. Viehauer *et al.*, Nucl. Instrum. Methods Phys. Res., Sect. A **462**, 146 (2001).
7. R. A. Briere *et al.* (CESR-c and CLEO-c Taskforces, CLEO-c Collaboration), Cornell University, LEPP Report No. CLNS 01/1742 (2001) (unpublished).
8. J. L. Siegrist *et al.*, Phys. Rev. D **26**, 969 (1982); A. E. Blinov *et al.* Z. Phys. C **49**, 239 (1991); A. E. Blinov *et al.* Z. Phys. C **70**, 31 (1996); Z. Jakubowski *et al.*, Z. Phys. C **40**, 49 (1988); C. Edwards *et al.*, SLAC-PUB-5160 (1990); R. Ammar *et al.*, Phys. Rev. D **57**, 1350 (1998).
9. J. H. Kühn, M. Steinhauser and T. Teubner, arXiv:0707.2589 [hep-ph].
10. S. Eidelman *et al.*, Phys. Lett. B **593**, 1 (2004).
11. M. Bethke, Nucl. Phys. Proc. Suppl. **135**, 345 (2004).
12. Q. He *et al.*, Phys. Rev. Lett. **95**, 121801 (2005) (Erratum-ibid. **96**, 199903 (2006)); J. Alexander *et al.*, arXiv:0801.0680 [hep-ex].
13. W.-M. Yao, *et al.*, Journal of Physics G **33**, 1 (2006).
14. E. Eichten, “New States above Charm Threshold,” talk presented at the International Workshop on Heavy Quarkonium, Brookhaven National Laboratory, June, 2006, and private communication.
15. F. E. Close and P. R. Page, Phys. Lett. B **628**, 215 (2005).
16. D. Ebert, R. N. Faustov and V. O. Galkin, Phys. Lett. B **634**, 214 (2006); L. Maiani, V. Riquer, F. Piccinini and A. D. Polosa, Phys. Rev. D **72**, 031502(R) (2005).
17. E. A. Kuraev and V. S. Fadin, Sov. J. Nucl. Phys. **41**, 466 (1985) (Yad. Fiz. **41**, 733 (1985)).
18. A. Osterheld *et al.*, SLAC-PUB-4160 (1986).